JOURNAL OF MATERIALS SCIENCE 32 (1997) 6343–6356

Toughening of polystyrene by natural rubber-based composite particles

Part II *Influence of the internal structure of PMMA and PS-grafted core-shell particles*

M. SCHNEIDER, T. PITH*, M. LAMBLA†
Ecole d'Application des Hauts Polymères, Institut Charles Sadron (CRM-EAHP), 4, rue Boussingault, Strasbourg, France

This work was focused on the influence of the internal structure of natural rubber (NR)-based core-shell particles on the toughness of polystyrene (PS). Several emulsion polymerization processes were used to control the degree of grafting of the NR phase and the site of polymerization, which determines the final morphology of the prepared composite NR-based particles. PS subinclusions were introduced into the NR core in order to determine their influence on the deformation behaviour of PS.

A continuous extrusion process was adapted for the direct feeding of the wet NR-based latexes into the molten PS matrix. Impact testing indicated that core-shell particles based on NR containing a large number of small crosslinked PS subinclusions toughened PS most effectively. A very effective toughening agent is obtained if a hard shell of 25 wt% crosslinked PMMA surrounds the composite rubber particle. Grafting of NR chains during the subinclusion synthesis has to be avoided since a high rubber particle modulus is detrimental for craze nucleation in PS. From the fracture surface morphology the craze nucleating and stabilizing efficiency of composite NR particles having different morphologies or grafting degrees could be deduced.

1. Introduction

A well-established means to improve the toughness of brittle polymers is to incorporate a dispersed rubber phase in order to improve the impact strength [1–3]. The major toughening mechanisms are crazing and shear yielding which allow polymers to absorb more energy at impact since the matrix is deformed more extensively. High impact polystyrene (HIPS) which contains rubber particles with polystyrene (PS) inclusions is toughened mainly by the nucleation and growth of crazes in the PS matrix [4, 5]. A possibility of obtaining very fine and well-defined morphologies consists of blending PS with core (rubber)-shell (hard polymer) latex particles of 0.1 to 5 μm [6]. These particles can be prepared by emulsion polymerization processes [7–10]. The toughening particles are crosslinked during their formation so that they retain their morphology during the blending process with PS and the subsequent moulding of the blends. This approach to rubber-toughened plastics allows an independent adjustment of the matrix properties and the composition and morphology of the dispersed rubber particles. Although toughening agents based on latex particles have been successfully commercialized by the company Röhm and Haas [11], there are only few publications [12] about the deformation behaviour and especially the influence of their morphology on the mechanical properties of blends containing such particles.

In a previous study, natural rubber (NR)-based core-shell latex particles have been examined as possible impact modifiers for polystyrene and polymethylmethacrylate (PMMA) [13, 14]. It was possible to adapt a continuous extrusion process in such a way that a wet latex could be fed directly into a twin-screw extruder. For example, even pure NR, or rubber particles containing PS subinclusions, and latex particles with very thin shells, which do not yield powders for the conventional weight feeders of polymer blending equipment, could be dispersed into a PS matrix. The latex particles act as stress concentrators and produce more extensive matrix deformation by crazing or shearing [15]. It was shown how the morphology of synthesized NR-based latex particles affects the

* Author to whom correspondence should be addressed.
† Deceased.

0022–2461

impact resistance of two polymers which deform either by crazing (PS) or by shear yielding (PMMA) [14]. We found that only core (natural rubber)-shell (crosslinked PMMA) particles toughened PMMA effectively. More complex latex particles containing PS subinclusions in the natural rubber core did not significantly improve the impact resistance of PMMA blends but proved to be essential for the impact reinforcement of PS blends which require at least three times bigger particles for effective polymer reinforcement. Comparing occluded natural rubber-based core-shell particles with latexes containing the same amount of hard polymer and rubber suggested that the deformation mode of the matrix polymer must have been changed and the influence of PS subinclusions which cause rubber fibrillation was studied in more detail.

This work was focused on the influence of the internal morphology of composite NR-based latex particles on the toughness of polystyrene. In order to be suitable for the reinforcement of a PS matrix, NR-based particles were coated with a shell of PMMA. Redox systems were used to control the site of the polymerization and thereby determine the final morphology of the prepared composite NR-based particles. Having established the optimal shell thickness for the toughened PS blends, different amounts of hard PS subinclusions were introduced into the rubber core. The emulsion polymerization procedures used for the preparation of these composite latex particles determine whether the NR chains will be grafted or not [16, 17]. This difference is due to the grafting mechanism which is based on a direct initiator attack on the natural rubber molecule. For example, due to poor resonance stabilization, azobisisobutyronitrile (AIBN) initiated polymerization produces virtually no graft polymer. Depending on the degree of grafting, NR-based particles of identical morphology can yield either tough or brittle PS blends. For each type of toughening particle the morphology actually obtained was checked by transmission electron microscopy (TEM).

Natural rubber as the core polymer in latex particles has an overall balance of properties which is unmatched by synthetic elastomers. Besides, NR is an alternative to synthetic impact modifiers because of its botanical and hence, renewable origin.

2. Experimental procedure

2.1. Materials

The PS matrix Lacqrène 1240 (M_n = 154 700; M_w = 357 600; M_z = 601 700; T_g = 100 °C) was kindly donated by Elf Atochem. A centrifuged natural rubber latex (Revertex AR) supplied by Revertex Ltd. was used as a seed latex in a sequential emulsion polymerization. The detailed emulsion polymerization technique for the preparation of the toughening composite natural rubber latexes has been described elsewhere [18]. Several initiation systems were used to control the degree of grafting of the NR phase and the site of polymerization which determines the final morphology of the prepared composite NR-based particles [19]. The extremely polydisperse particle size distribution curve of a typical composite natural rubber latex is plotted in Fig. 1 as obtained by photon correlation spectroscopy performed on a Malvern Autosizer II.

The *z*-average particle size of the natural rubber seed latex is 530 nm. The glass transition temperature of natural rubber lies at −60 °C. Fig. 2 is a typical scanning electron photomicrograph (SEM) of the composite NR-based particles containing 30 wt % crosslinked PS subinclusions and 25 wt % crosslinked PMMA in the shell of the particle. Polydisperse and hard particles are clearly visible. Twenty-five per cent by weight of crosslinked PMMA in the particles are sufficient to form a closed shell around the NR/PS semi-interpenetrating network (semi-IPN) core in order to obtain isolated particles. In fact, the shell polymer concentration could be decreased from 40 wt % crosslinked PMMA in case of crosslinked NR based particles [13] to only 25% in order to prevent the rubber particles from filmforming.

In order to promote a core-shell structure we used the bipolar redox initiator couple t-butyl hydroperoxide/tetraethylene pentamine (t-BuHP/TEPA) [20, 21].

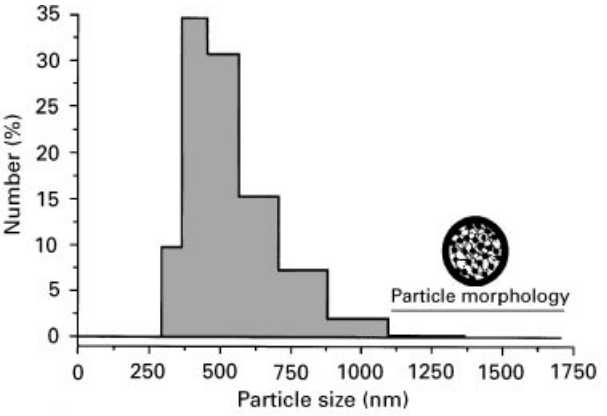

Figure 1 Size distribution curve of a composite NR-based latex containing 30 wt % crosslinked PS subinclusions in the core and 25 wt % crosslinked PMMA in the shell of the particles.

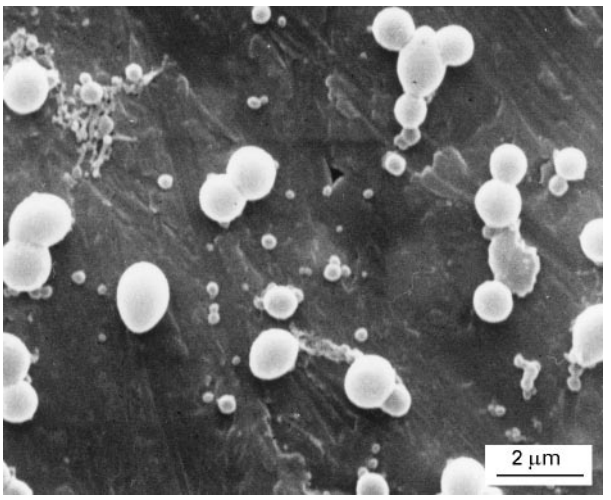

Figure 2 SEM photomicrograph of composite NR-based latex particles containing 30 wt % crosslinked PS subinclusions in the core and 25 wt % crosslinked PMMA in the shell.

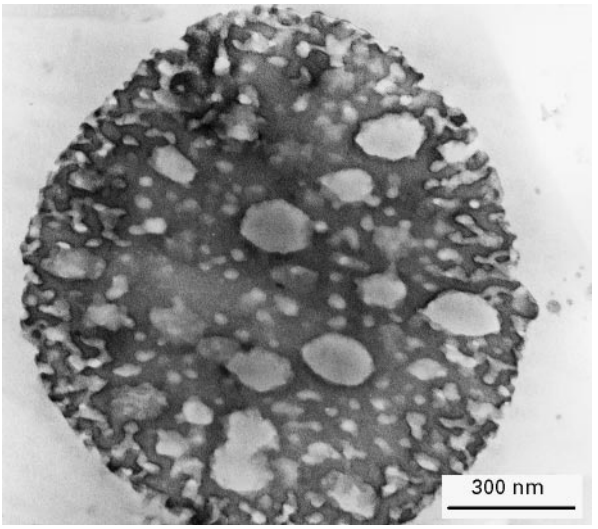

Figure 3 TEM photomicrograph of the ultramicrotome cut of a composite NR based latex particle containing 30 wt % crosslinked PS subinclusions in the core and 25 wt % crosslinked PMMA in the shell (core-synthesis: AIBN initiation, shell-synthesis: bipolar redox system).

In this case, most of the free radicals are produced at the monomer swollen particle/water interface, taking into account the fact that the peroxide is soluble in the organic phase, whereas the activator tetraethylene pentamine is water soluble. On the other hand, the formation of crosslinked PS subinclusions within the NR seed latex particles results from the initiation induced by AIBN, which does not graft NR, or the lipophilic redox system t-butyl hydroperoxide/dimethylaniline (t-BuHP/DMA) which grafts NR. The polymerization takes place entirely within the monomer swollen NR latex particles. Fig. 3 shows an example of the morphology that is obtained by polymerizing first styrene and then methylmethacrylate in the presence of an uncrosslinked NR seed latex; it is a TEM photomicrograph of an osmium tetroxide-stained NR-based particle that contains 30 wt % crosslinked PS in subinclusions within the NR core and 25% crosslinked PMMA in the shell region. The hard PS subinclusions were sythesized by AIBN initiation at 70 °C.

The TEM photomicrograph in Fig. 3 shows clearly that the styrene monomer polymerized in microdomains within the NR seed latex. Most of the secondary polymer resides in 200–250 nm sized subinclusions. Very small inclusions (< 50 nm) can also be seen. The 40 wt % crosslinked PS/60 wt % NR latex semi-IPN particles were subsequently coated with PMMA using the bipolar redox initiation system. It is not possible to exclude the possibility that some of the PMMA (25 wt % in the particle) polymerized within the nucleus of the semi-IPN seed latex particles. A 100–200 nm thick intermeshed interface region between the PS/NR latex semi-IPN based core and the PS matrix can be clearly distinguished. A perfect PMMA shell could not be achieved but the PMMA meandered into the NR/crosslinked PS latex semi-IPN core. A similar morphology resulted for the grafted NR/crosslinked PS latex semi-IPN based particles which were sythesized by redox initiation at low temperature.

TABLE I Summary of the natural rubber-based composite particle characteristics

Latex	Core composition	Shell composition	Core/shell ratio
NR	Natural rubber	–	–
	Natural rubber	Crosslinked PMMA	75/25
	Natural rubber	Crosslinked PMMA	60/40
	80% natural rubber/ 20% crosslinked PS	–	–
	60% natural rubber/ 40% crosslinked PS	–	–
	80% natural rubber/ 20% crosslinked PS	Crosslinked PMMA	80/20
	80% natural rubber/ 20% crosslinked PS	Crosslinked PMMA	75/25
	80% natural rubber/ 20% crosslinked PS	Crosslinked PMMA	60/40
	60% natural rubber/ 40% crosslinked PS	Crosslinked PMMA	75/25
	40% natural rubber/ 60% crosslinked PS	Crosslinked PMMA	75/25

A PS shell was much more difficult to produce when the bipolar redox system and a semicontinuous emulsion polymerization procedure were used. A large fraction of the monomer polymerized in very small microdomains within the NR core. The subinclusions of such latex particles which contain 40 wt % crosslinked PS are about 30 nm in diameter. Their size is at least six times smaller than in the case of the AIBN batch synthesis at 70 °C [18].

Characteristic data on the natural rubber based composite latex particles used are summarized in Table I. The schematically represented morphology of the latex particles was verified by TEM observation. If not specified otherwise, all secondary polymers contained 0.25 wt % ethylene glycol dimethacrylate (EGDMA) as crosslinking agent. In the case of the shell synthesis the bipolar redox initiation system cosisting of t-butyl hydroperoxide and tetraethylene pentamine was used for all composite latexes. The PS subinclusions were usually sythesized by the AIBN initiation at 70 °C. In some cases, which each time are specified in the text or in the figure legend, the temperature was raised to 85 °C or the lipophilic redox system t-butyl hydroperoxide/dimethylaniline was used at 50 °C.

2.2. Blend preparation

The set-up for the addition of a wet latex directly into a co-rotating ZSK 30 Werner & Pfleiderer twin-screw extruder, which is schematically shown in the first part of this series [13], was used for the continuous blend preparation of all PS blends investigated. It is important to note that a co-rotating twin-screw extruder is

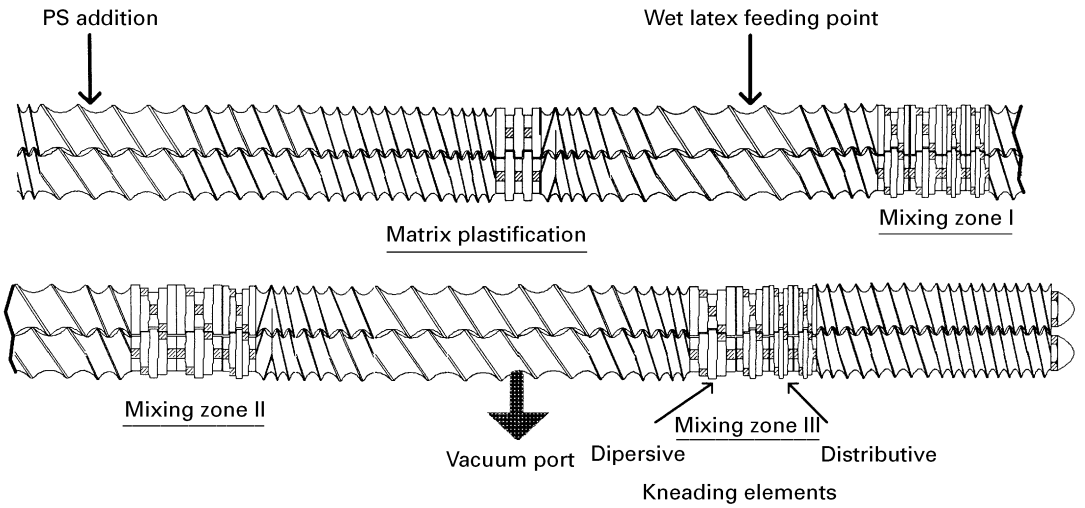

Figure 4 Screw configuration used for continuous blend preparation.

self-wiping and any traces of the polymer which may otherwise remain dormant in the extruder are removed. This is particularly significant since NR is especially sensitive to degradation by heat and oxygen. No antioxidants were used. Fig. 4 gives a detailed overview of the chosen screw configuration.

All elements on a screw convey and mix. The major effect depends on the design of the screw elements which have been classified into conveying elements and mixing elements. If kneading discs are staggered in the same sense as the conveying elements, they are said to have a forward configuration. They have a backward configuration when the kneading discs are staggered in the opposite sense. A kneading block with a neutral configuration followed by a short conveying element with a reverse flight just before the wet latex addition ensured that the PS matrix was completely plastified at the feeding point. The reverse conveying element acted as a mechanical barrier which prevented unmelted particles from going downstream. Three mixing zones consisting of first dispersive and then distributive mixing elements with a forward configuration helped to distribute the particles uniformly into the PS matrix. Mixing zone II is followed by a reverse conveying element in order to fill up the channel around the block. This configuration provided a "melt seal" in order to establish a constant vacuum pressure in the following degassing section of the barrel. Furthermore, it ensured that the vacuum did not affect the polymer flow in other sections of the screw. The extrusion process was performed at a throughput of $5\,kg\,h^{-1}$, 150 r.p.m. and 210 °C. Different amounts of the wet latexes were fed into the extruder in order to obtain various mass fractions of the composite rubber particles within the PS matrix without changing throughput or processing temperature.

2.3. Mechanical tests

ASTM test samples were moulded on a Billon 150/150 injection moulding machine at 210 °C and left at 23 °C and 50 % relative humidity for 1 week.

The Izod impact resistance of V-notched samples (based on ASTM D256) was obtained using a standardized Zwick pendulum impact testing machine. The bar dimensions were $63 \times 12.8 \times 6$ mm. Tensile testing on dumbbell samples (based on ASTM D638) was performed on a hydraulic Instron 8031 machine at room temperature. The elongation (strain rate $50\,mm\,min^{-1}$) was measured directly on the sample by a tensometer.

2.4. Electron microscopy

A Cambridge Instruments Stereoscan 120 scanning electron microscope was used for the examination of the latex sample in Fig. 2 which was prepared in the following way. A diluted drop of latex was put onto an aluminium support and subsequently put into liquid nitrogen. Then a gold layer was deposited on the still frozen support with a Cambridge Instruments sputter coater. Izod fracture surfaces of the prepared blends were coated by gold vapour deposition before viewing.

A Philips EM 300 transmission electron microscope was used in order to observe ultramicrotome sections of the PS blends which were prepared in the following way. First a smooth surface of the PS blend was exposed to osmium tetroxide vapours during 48 h in order to stain the NR phase [22, 23]. The staining not only enhanced the contrast for the microscopic viewing of the blends but also hardened the rubber phase. In this way ultramicrotome sections could be prepared without altering the particle morphology of the no longer soft rubber particles.

3. Results and discussion

3.1. Blend preparation

In the first part of this series [13] it was shown that pure NR particles could be dispersed into the PS matrix when the tacky rubber particles were fed as a wet latex directly into the extruder. In order to ensure that the NR based particle morphology did not change during the blending process, the morphology of a PS blend with 20 wt % tacky natural particles containing 40 wt % PS subinclusions was also checked.

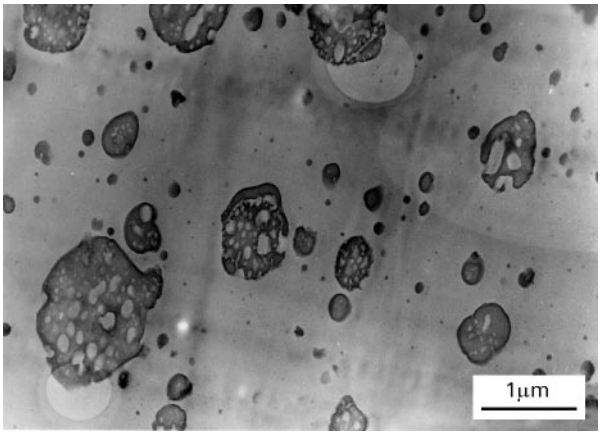

Figure 5 TEM photomicrograph of a PS blend with 20 wt % natural rubber particles containing 40 wt % crosslinked PS subinclusions.

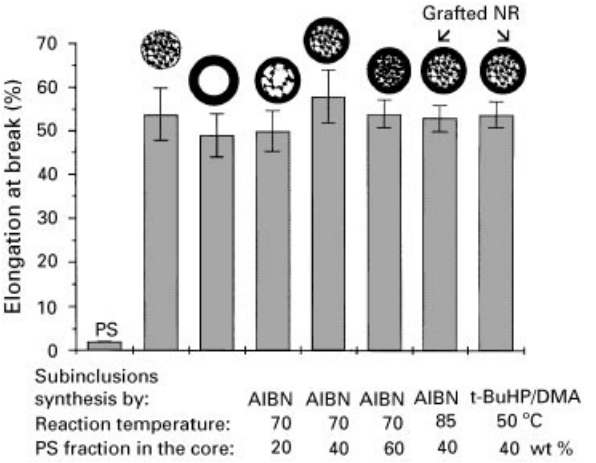

Figure 6 Comparison of the elongation at break of PS blends containing 27 wt % composite latex particles based on different NR/crosslinked PS semi-IPNs.

The transmission electron photomicrograph in Fig. 5 confirms once more the integrity of tacky rubber particles after the mixing process. Of course, it is easier to distribute hard particles within a polymer since they cannot stick together. It can be seen that even at high particle mass fractions in the blend, particle collisions did not cause any particle agglomeration. Of course, hard particles can also be fed as a free flowing powder as in conventional blend preparation processes [14].

3.2. Tensile testing

High deformation speeds (impact testing) were necessary in order to evaluate the mechanical properties of PS blends with a series of the prepared structured latexes. The composite NR-based particles are represented schematically above the corresponding bar graphs in Fig. 6.

High reaction temperature (85 °C) or the redox system consisting of t-BuHP/DMA yield grafted semi-IPNs. Comparing the elongation at break of PS blends containing composite NR-based particles with different amounts of PS subinclusions or latexes with the same amount of PS subinclusions, but different degrees of grafting, did not show any differentiation between the different latex particles.

3.3. Shell thickness

Both subinclusions within the rubber phase and a PMMA shell are necessary for effective rubber toughening of PS at fast deformation speeds (ASTM based impact testing) [13]. In order to study the effectiveness of core-shell particles containing subinclusions these two factors have to be analysed separately. It is not possible to exclude the possibility that no subinclusions are formed within the nucleus of a core-shell particle during the shell synthesis by emulsion polymerization. However, subinclusions can be formed within the nucleus of rubber particles which are not grafted at the surface. Different amounts of the shell forming polymer PMMA were subsequently introduced into the particles in order to determine the optimal shell thickness.

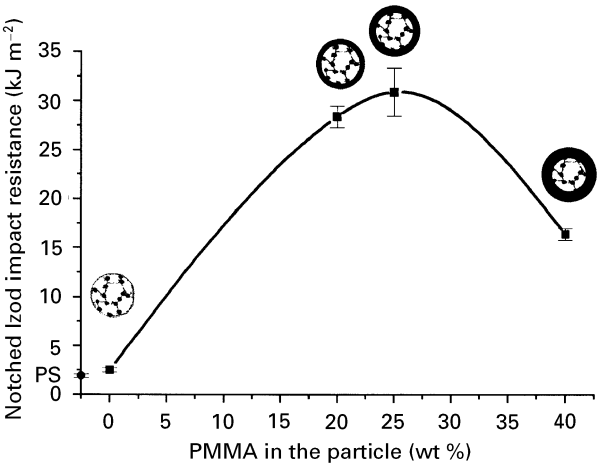

Figure 7 Impact resistance of PS blends with 27 wt % natural rubber/PS (60/40) based particles containing 0, 20, 25 and 40 wt % crosslinked PMMA in the shell.

Fig. 7 indicates that NR rubber particles containing 40 wt % crosslinked PS subinclusions and no hard shell did not offer any impact improvement to PS. This result is very significant since it demonstrates that subinclusions alone do not render rubber particles capable of reinforcing PS. It is clear that at high deformation speeds occluded rubber particles without an outer grafted hard layer cannot initiate a large number of crazes and at the same time control craze breakdown in order to avoid premature failure. A hard shell plays the crucial role. Additional subinclusions improve rubber fibrillation at impact and thus impede more effectively the degeneration of crazes into a running crack, thus allowing more matrix deformation and energy absorption. At slow deformation speeds (tensile testing) the matrix polymer chains of the PS matrix can respond readily to the tensile stress by the formation of highly oriented craze matter. Fig. 6 shows that a hard shell or rigid subinclusions were equally effective. Even pure rubber particles allowed the matrix to be elongated to more than 25 %; it is known that they increased the stress intensity at the particle equator. It is known that

different loading rates influence the toughening mechanism; for example, fibril structure and thickness due to fibril coalescence are altered [24].

Fig. 7 establishes that 25 wt % of crosslinked PMMA in the particles is the optimal amount for the formation of a complete shell. Higher PMMA mass fractions in the composite particles (e.g. 40 wt %) reduced the impact resistance. This might be explained by the increased particle modulus which decreases the effectiveness of toughening agents [25, 26]. Besides, the redox initiation system used for the shell synthesis grafts the natural rubber chains which further reduced the effectiveness of the incorporated rubber particles. It has to be taken into account that the polymer blends, which are reinforced by latex particles with thicker PMMA shells, contained less natural rubber since part of the rubber is substituted by PMMA. Less than 25 wt % crosslinked PMMA in the particles is not sufficient to form an entire shell around the NR/PS semi-IPN core. In fact, the complex emulsion polymerization procedure used produces imperfect core-shell particles, but the polar secondary polymer could only be concentrated in the shell region of the NR based particles, as shown in Fig. 3. Considerable amounts of PMMA had to be introduced into the latex particle in order to form a complete shell.

The Izod fracture surface of a PS blend containing occluded natural rubber particles with and without a very thin PMMA shell is shown in Figs 8 and 9. The thin crosslinked PMMA shell represents only 20 % of the particle mass.

It is clear that occluded rubber particles without a PMMA shell did not initiate stable crazes in the PA matrix. Fig. 8 reveals a brittle fracture surface without any matrix deformation. No stress transfer to the occluded rubber phase was possible and most of the incorporated particles debonded from the matrix at impact. The few micrometer sized particles which are present in the very polydisperse natural rubber latex fractured in preference to debonding from the matrix. A model of Bucknall and co-workers [25, 26] explains that large sized rubber particles are easier to cavitate at impact. Therefore no holes of debonded particles larger than 0.9 μm could be found.

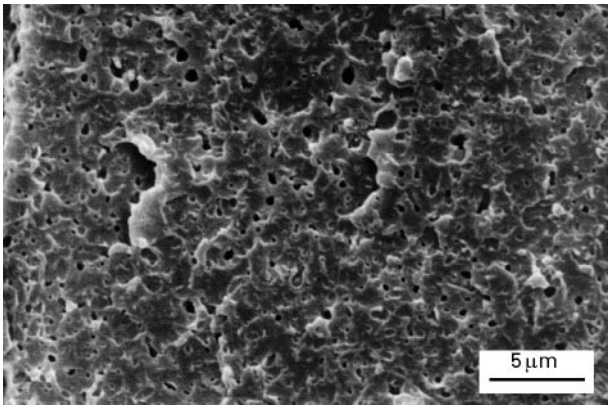

Figure 8 Scanning electron micrograph of the notched Izod fracture surface of a PS blend with 27 wt % natural rubber particles containing 40 wt % crosslinked PS subinclusions.

A very thin PMMA shell was able to transform ineffective occluded rubber particles into a very efficient toughening agent. No debonded particles could be found and a fracture surface with a profuse array of crazes is visible in Fig. 9.

3.4. Natural rubber/PS subinclusions ratio in the core

3.4.1. Impact resistance

Having established the optimal shell thickness, the role of hard PS subinclusions within the rubber core on the fracture toughness of PS blends could be analysed in detail. First, the PS/NR ratio in the core was varied and the measured impact resistance of PS blends containing these particles is plotted in Fig. 10.

The fracture toughness deteriorated when the mass fraction of the subinclusions in the core was raised from 20 to 40 or 60 wt %. The increased volume fraction of the rubber phase in the blend which generally improves the impact strength of rubber-toughened polymers might be counterbalanced by an increased

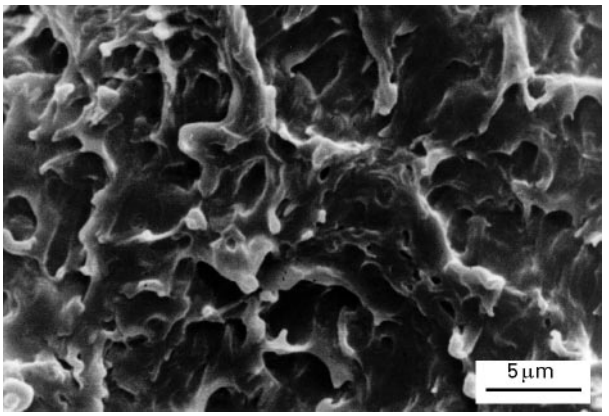

Figure 9 Scanning electron micrograph of the notched Izod fracture surface of a PS blend with 27 wt % natural rubber-based particles containing 15 wt % crosslinked PS subinclusions and 20 wt % crosslinked PMMA in the shell.

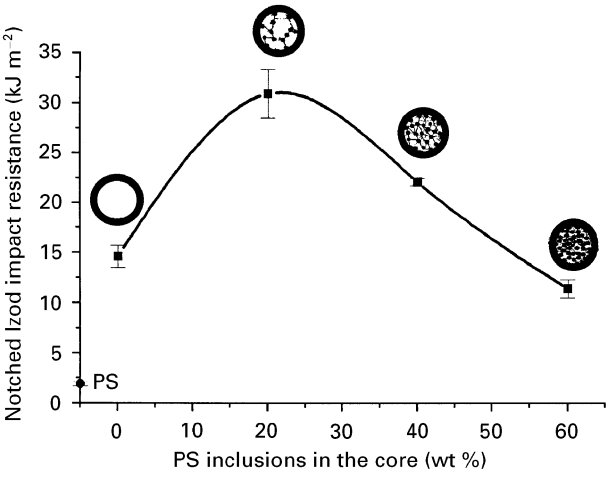

Figure 10 Impact resistance of PS blends with 27 wt % NR-based core-shell particles containing 0, 15, 30 and 45 wt % crosslinked PS subinclusions in the natural rubber core and 25 wt % crosslinked PMMA in the shell.

modulus of the rubber particles. It is known from literature [1, 25, 26] that an increased modulus of rubber particles reduces the effectiveness of rubber particles to initiate crazes. Another explanation of this behaviour can be given when the occluded rubber core is observed by TEM. In fact, the large sized PS subinclusions within the natural rubber core which are presented in Fig. 3 diminished only in size when the PS mass fraction in the particle was decreased [18]. The distribution and number of the PS occlusions within the rubber phase did not change. Since higher PS mass fractions increased only the subinclusion size, their efficiency to fibrillate the rubber core at impact is not changed. This effect can be validated when the impact resistance is correlated with the rubber weight fraction in the prepared blends.

Fig. 11 shows that the impact resistance of PS blends containing the same mass fraction of core-shell particles but different amounts of crosslinked PS subinclusions in the NR core was controlled only by the rubber weight fraction in the blend. The linear dependence proves that bigger occlusions within the natural rubber phase did not change the rubber fibrillation and the crazing mechanism of the PS matrix. Rigid crosslinked PS subinclusions within the core-shell particles constrain the low modulus rubber phase that separates them, allowing the natural rubber to break up into fibrils. Increasing the size of the subinclusions did not alter this mechanism. Larger sized PS subinclusions did not make more effective use of the natural rubber. In fact, our results corroborate the findings of Donald and Kramer [27, 28] who concluded that the toughest HIPS must contain rubber particles with a large number of small PS occlusions. Of course, their particles contained an exterior PS grafted hard shell. PS blends containing core-shell particles without subinclusions could not be correlated with the mechanical properties of blends containing occluded core-shell particles. The rubber particle fibrillating and cavitation mechanisms in these PS blends, which have been investigated further [29], had changed.

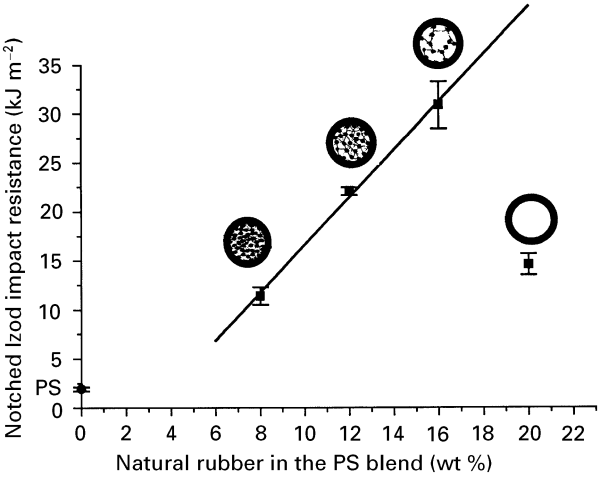

Figure 11 Correlation of the impact resistance of PS blends with the natural rubber weight fraction in the incorporated 27 wt % core-shell particles containing 0, 15, 30 and 45 wt % crosslinked PS subinclusions within the rubber core (core/shell ratio: 75/25).

Examination of Izod fracture surfaces of the prepared PS blends with NR based composite particles containing 30 or 45 wt % PS subinclusions in the rubber core and 25 wt % crosslinked PMMA in the shell confirmed these findings.

Figs 12 and 13 show that subinclusions prevented a decohesion of the incorporated composite particles from the PS matrix. No holes of debonded particles are visible. At the same particle content in the blend, a higher mass fraction of crosslinked PS within the rubber core led to a smaller volume of plastic deformation.

3.4.2. Tensile behaviour

The effects of the core NR/crosslinked PS weight ratio on the yield stress of the prepared PS blends were also studied at slow deformation rates. Fig. 14 compares the effectiveness of core-shell particles with different amounts of crosslinked PS subinclusions in decreasing the yield stress of the prepared PS blends.

The composition of the NR/crosslinked semi-IPNs in the core influences the stress–strain properties less than the impact resistance of the prepared PS blends.

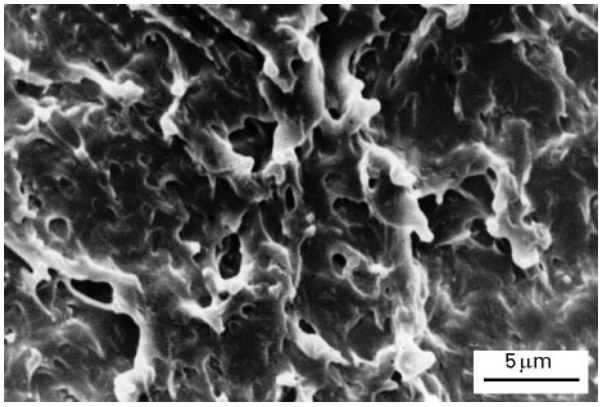

Figure 12 SEM photomicrograph of the notched Izod fracture surface of a PS blend with 27 wt % core-shell particles containing 30 wt % crosslinked PS subinclusions in the core and 25 wt % crosslinked PMMA in the shell.

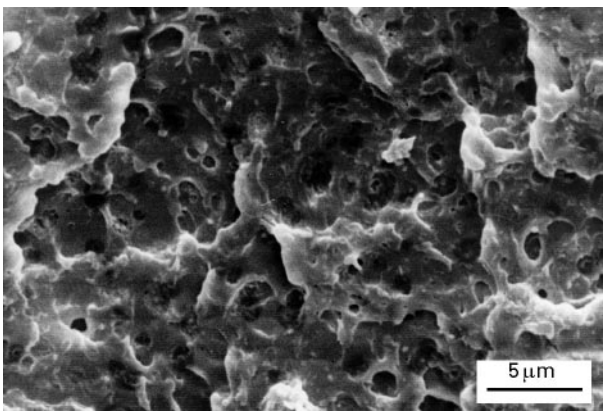

Figure 13 SEM photomicrograph of the notched Izod fracture surface of a PS blend with 27 wt % core-shell particles containing 45 wt % crosslinked PS subinclusions in the core and 25 wt % crosslinked PMMA in the shell.

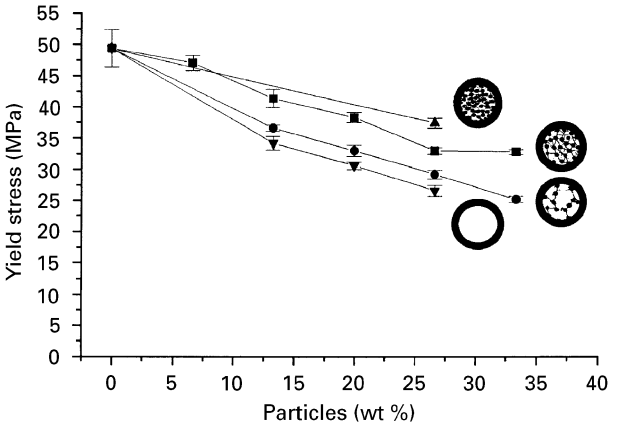

Figure 14 Correlation of the yield stress of PS blends containing different weight fractions of core-shell particles containing 0, 15, 30, 45 wt % crosslinked PS subinclusions in the rubber core and 25 wt % crosslinked PMMA in the shell.

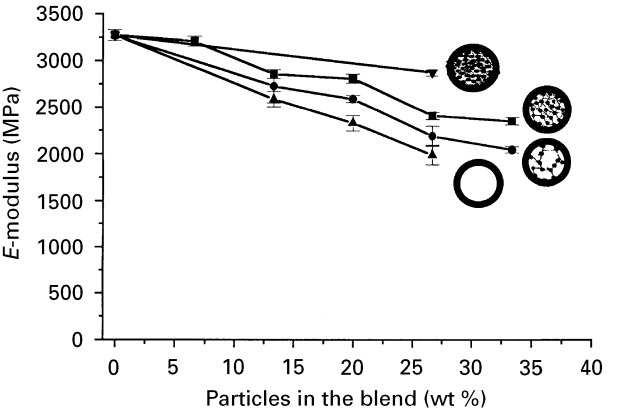

Figure 15 Correlation of the *E*-modulus of PS blends with different weight fractions of core-shell particles containing 0, 15, 30 and 45 wt % crosslinked PS subinclusions in the natural rubber core and 25 wt % crosslinked PMMA in the shell.

Higher core PS/natural rubber weight ratios increased the yield stress of the PS blends because the increased modulus of the incorporated particles shifts to higher stresses the rubber cavitation preceding crazing [26]. Both more PS subinclusions and grafting of the natural rubber chains increased the particle modulus. Despite the use of AIBN initiation for the preparation of the NR/crosslinked PS semi-interpenetrating networks, the possibility of grafting cannot be completely excluded. It is generally accepted that AIBN initiation does not promote grafting of styrene onto natural rubber, since AIBN cannot abstract hydrogen atoms from the NR backbone [30, 31]. However, a recent publication [32] stated that NR chains had indeed been grafted.

The composition of the composite NR particles determines not only the stress concentration in the surrounding matrix but also the modulus of the rubber modified polymer. Fig. 15 compares the *E*-modulus of PS blends containing core-shell particles with different amounts of crosslinked PS subinclusions.

Increasing the PS mass fraction in the rubber core from 20 to 40 or 60% increased the modulus of the rubber-modified PS blends. A linear dependence can be established for the *E*-modulus/particle content relationship. The composite latex particles presented in Fig. 15 contained less rubber because part of it was substituted by the PS subinclusions within the NR core. Consequently a higher Young's modulus has to be expected in PS blends with these particles. However, the influence of the composition of the particles on the blend modulus is less pronounced than their influence on the impact resistance.

Fig. 16 gives a typical example of the dependence of the elongation at break of PS blends on the content of core-shell particles containing 15 and 30 wt % crosslinked PS subinclusions in the rubber core and 25 wt % crosslinked PMMA in the shell. Furthermore, the elongation at break of PS blends with NR particles containing 40 wt % crosslinked PMMA in the shell are plotted in Fig. 16. The simple core-shell particles comprise as much secondary polymer as the

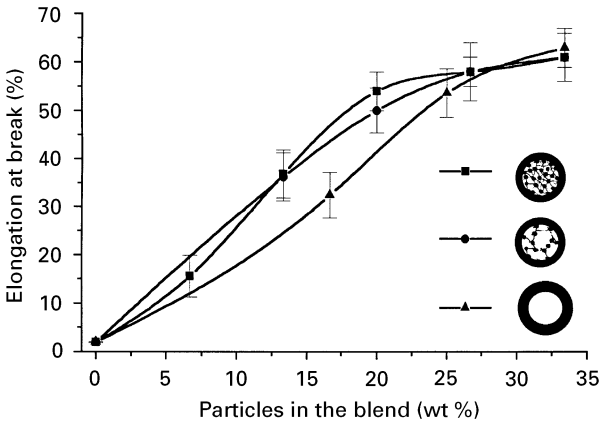

Figure 16 Example of the dependence of the elongation at break of PS blends with different mass fractions of core-shell particles containing 0, 15 and 30 wt % PS subinclusions in the rubber core (25 wt % crosslinked PMMA in the shell of occluded core-shell particles, 40 wt % crosslinked PMMA in the shell of simple core-shell particles).

core-shell particles containing 15 wt % PS subinclusions within the rubber core.

The elongation at break of all three PS blends reached a saturation value of 60% at high particle contents. Fig. 16 indicates that PS blends containing core-shell particles with hard PS subinclusions can be deformed more extensively by crazing at particle mass fractions below 20 wt %. The subinclusions permit the rubber core to fibrillate more readily which accomodates the displacement of the surrounding craze and prevents premature failure of the sample. Occluded NR-based core-shell particles containing the same mass fraction of secondary polymers as simple core-shell particles are clearly superior. A direct comparison is possible since these two PS blends contained the same rubber mass fraction.

3.5. Crosslinking degree of the PS subinclusions

After studying the effects of composite NR particles with different morphologies on the toughness of PS

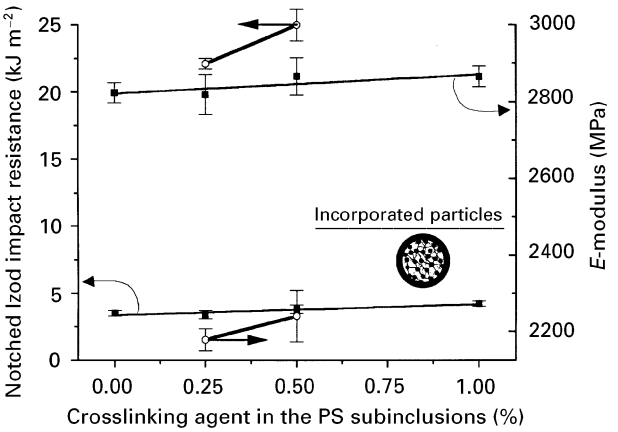

Figure 17 Dependence of the mechanical properties of PS blends on the weight fraction of crosslinking agent in the PS subinclusions within the incorporated core-shell particles containing 30 wt % PS and 25 wt % crosslinked PMMA in the shell. (■) 13 wt %; (○) 27 wt %.

blends, the chemical and physical properties of the rubber core have to be considered too. First, the degree of crosslinking in PS subinclusions within uncrosslinked NR rubber particles was varied. The particles always contained an optimal amount of crosslinked PMMA in the shell for most effective reinforcement. In Fig. 17 the resulting mechanical properties of the obtained blends are correlated with the amount of EGDMA (crosslinking agent) in the PS subinclusions. A series of dilute PS blends containing 13 wt % particles were prepared. Furthermore, two blends were analysed at high particle mass fractions (27 wt %) in order to study high impact PS blends too.

Both *E*-modulus and impact energy depend linearly on the amount of crosslinking agent in the PS subinclusions. The effect is more pronounced in the case of high impact blends. A low degree of crosslinking of latex interpenetrating networks implies that the elastic–retractile force does not exceed the sum of the mixing and interfacial forces during emulsion polymerization and large spherical inclusions result within the particle [33]. In the case of the NR crosslinked PS semi-IPNs an increased crosslinking density promoted phase separation of the PS subinclusions within the rubber phase. Similar effects of the degree of crosslinking on phase separation in bulk interpenetrating networks are known [34]. The decreased size of the subinclusions within the NR core might be one reason for the better mechanical properties. The observed morphological change of the toughening agent could have enhanced the rubber fibrillation which prevents craze failure more effectively, as already known from literature [27, 28].

This finding is in accordance with the results presented in Fig. 10 where smaller PS mass fractions in the core led to an improved impact resistance of the prepared PS blends. Changing the degree of crosslinking in the hard PS subinclusions which are dispersed within the rubber phase influenced the performance of the impact modifier mainly by a change of the morphology of the semi-IPN core. However, emulsion polymerization procedures have a greater impact on the morphology of the prepared composite latex particles. Not simply a few large subinclusions in the rubber core, but many small subinclusions, are needed for most effective rubber fibrillation and cavitation at impact. For example, a semicontinuous feeding process leads to a decrease of the PS subinclusion size by a factor of six in relation to a batch process polymerizing the same amount of styrene monomer in a natural rubber seed latex [18]. It is the morphology of the toughening particles which controls predominantly the mechanical properties of PS blends with such particles.

3.6. Polymerization temperature for the subinclusion synthesis

The preparation of PS subinclusions within a NR core by AIBN initiation at 70 °C takes 5 h, which is very long compared to conventional emulsion polymerization procedures. A rise of 15 °C of the reaction temperature allows the reaction to finish within 2 h. However, chain transfer to the NR macromolecules is enhanced by the rise of temperature since grafting reactions have a higher activation energy than homopolymerization [35–37].

Figure 18 presents the impact resistance of PS blends with natural rubber based core-shell particles containing 40 wt % crosslinked PS subinclusions which were prepared at 85 °C (grafted NR) or 70 °C (not grafted NR). Composite toughening particles prepared by AIBN initiation at 85 °C began to reinforce PS only at particle mass fractions exceeding 25%. Grafted NR based particles could not toughen the matrix polymer at fast deformation rates. This finding is in accordance with literature [38] which established that high modulus particles are less effective in nucleating a large number of crazes in PS. In fact, the ratio of particle modulus to matrix modulus must be below 0.3 for effective rubber toughening to take place [39]. Furthermore, the minimum particle size for craze nucleation is raised when the particle modulus is

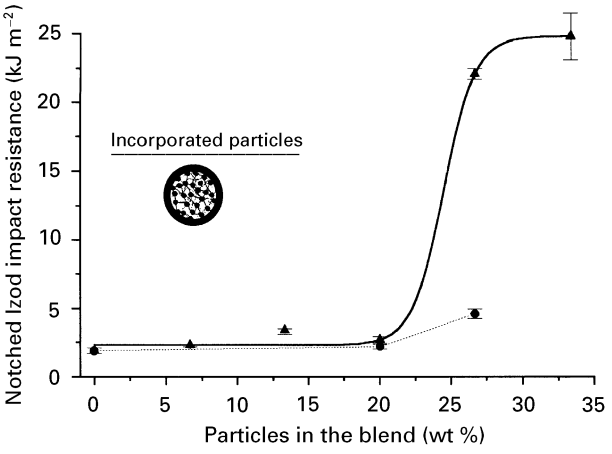

Figure 18 Dependence of the impact resistance of PS blends on the reaction temperature used for the synthesis of 30 wt % PS crosslinked subinclusions within the incorporated NR-based latex particles containing 25 wt % crosslinked PMMA in the shell. (▲) non-grafted IPN (synthesis at 70 °C); (●) grafted IPN (synthesis at 80 °C.

increased [40]. This means that the small particles of the used very polydisperse NR latex whose particle size distribution curve is plotted in Fig. 1 were ineffective and more particles had to be incorporated before the impact resistance began to rise.

Grafting reactions are not the only factors to be considered. The reaction temperature also influences the morphology of the prepared composite latex particles [18]. A high reaction temperature caused an increase of the subinclusion size since the viscosity within the latex particles is lower during high temperature emulsion polymerization. The adverse effect of large subinclusions on the toughening efficiency has already been described in earlier sections.

Lowering the reaction temperature for the synthesis of the PS subinclusions to 60 °C only slightly improved the reinforcement of the PS blends. The impact resistance rose from 22 kJ m^{-2} to 24 kJ m^{-2} when the subinclusion size was decreased [18]. Considering an overall reaction time of more than 20 h in this case, a possible industrial exploitation does not seem to be feasible. The reaction temperature should be raised as much as possible until excessive grafting renders the latex particles ineffective as toughening agents for PS.

3.7. Initiation systems for subinclusion synthesis

3.7.1. Impact resistance

Different initiation systems can be used for the preparation of PS subinclusions within a NR rubber core. Latex particles with the same morphological structure but different dynamic mechanical properties of the natural rubber phase result. For example, the use of the lipophilic redox system t-BuHP/DMA at 50 °C (peroxide initiation) leads to highly grafted rubber in contrast to AIBN initiation at 70 °C which generally does not graft the NR. Fig. 19 shows how essential it is to control the grafting degree of the NR phase.

PS blends containing grafted NR-based latex particles were not tough even at particle concentrations exceeding 25 wt %. Besides the reasoning of the preceding paragraph for the restricted toughening capacity of grafted, high modulus NR-based core-shell particles another explanation can be given when rubber cavitation is considered [25, 41–45]. As the modulus of the particles increases rubber cavitation, which precedes the crazing process, is retarded and the tensile stress needed for matrix deformation is too high. Hence, the few nucleated crazes fail and premature matrix fracture is caused.

Examination of Izod fracture surfaces of the prepared PS blends containing grafted NR/crosslinked PS semi-IPN networks-based core-shell particles indicates that this type of rubber particle cannot transform enough of the PS matrix into craze matter at fast deformation speeds.

Figs 20 and 21 show brittle fracture surfaces. Most of the particles debonded from the matrix and the crack did not go through the particles but went around them. The few micrometer sized particles which are present in the very polydisperse natural rubber latex

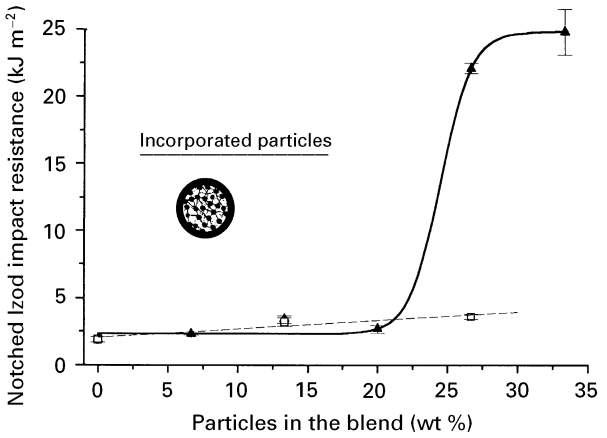

Figure 19 Dependence of the impact resistance of PS blends on the initiation systems used for the synthesis of 30 wt % crosslinked PS subinclusions within the incorporated NR-based latex particles containing 25 wt % crosslinked PMMA in the shell. (▲) non-grafted IPN (AIBN initiation); (□) grafted IPN (peroxide initiation).

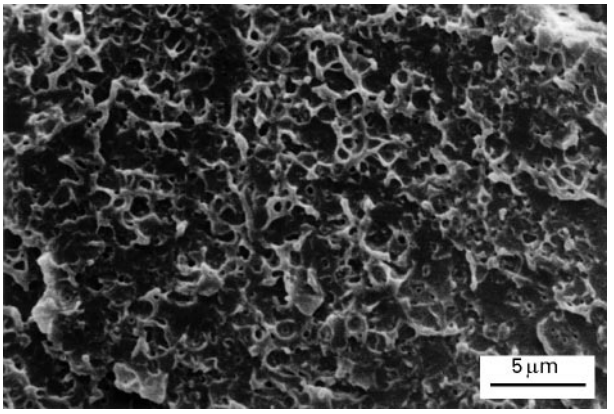

Figure 20 SEM photomicrograph of the Izod fracture surface of a PS blend containing 27 wt % core-shell particles based on 60 wt % NR/ 40 wt % crosslinked PS semi-IPNs prepared by AIBN initiation at 85 °C (core/shell ratio: 75/25, 30 wt % subinclusions in the rubber core).

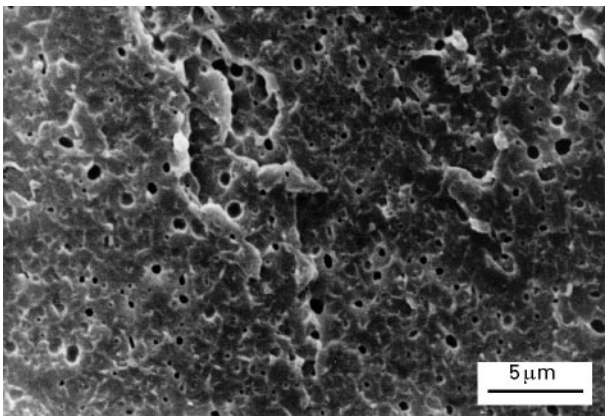

Figure 21 SEM photomicrograph of the Izod fracture surface of a PS blend containing 27 wt % core-shell particles based on 60 wt % NR/ 40 wt % PS semi-IPNs prepared by t-BuHp/DMA initiation at 50 °C (core/shell ratio: 75/25, 30 wt % subinclusions in the rubber core).

fractured in preference to debonding from the matrix. This can be explained by the fact that large sized particles are easier to cavitate. Fig. 20, which is a fracture surface of a PS blend containing 27 wt % latex

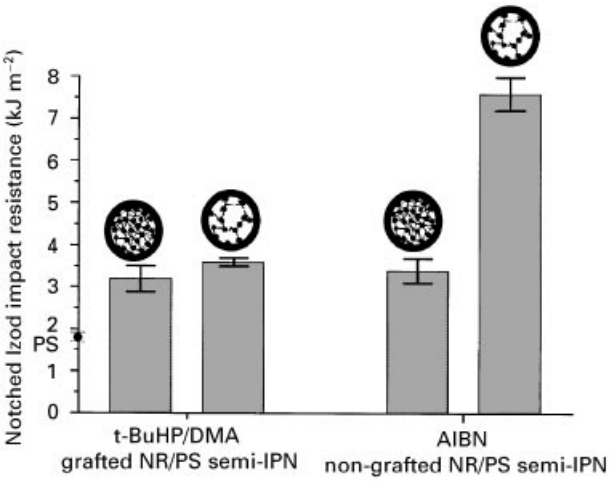

Figure 22 Dependence of impact resistance of medium impact PS blends on the degree of grafting of NR/crosslinked PS semi-IPN-based core-shell particles containing 15 or 30 wt % crosslinked PS subinclusions and 25 wt % crosslinked PMMA in the shell (13 wt % particles in the blends).

semi-IPN-based particles prepared at 85 °C, indicates that the matrix polymer begins to be transformed into crazed matter. This finding is in accordance with the impact resistance of PS blends containing these particles. Fig. 18 shows that the impact resistance of PS blends containing more than 27 wt % of this type of latex semi-IPN-based particles began to rise.

Comparing NR-based core-shell particles containing 15 or 30 wt % crosslinked PS subinclusions helped to distinguish further between grafted and non-grafted composite natural rubber particles. Fig. 22 summarizes the results of the impact resistance of different PS blends at a small particle mass fraction in the blend (13 wt %).

AIBN initiation, which is considered not to graft NR chains, produced NR/crosslinked PS semi-IPN-based core-shell particles containing 15 wt % PS subinclusions which toughened the PS matrix at only 13 wt % particles in the blend. Twice as much energy could be absorbed when non-grafted NR latexes are compared to grafted but morphologically identical rubber particles. Grafted NR-based core-shell particles did not significantly improve the stiffness of PS blends either because the modulus of the prepared blends was only slightly increased. NR/crosslinked PS-based core-shell particles containing 30 wt % subinclusions did not yet toughen the matrix polymer at small particle contents. It appears that increased particle modulus greatly reduced their toughening effectiveness. The morphology of the notched Izod fracture surfaces gives an indication of the deformation mechanisms of PS blends containing grafted (Fig. 23) and non-grafted (Fig. 24) NR/PS semi-IPN-based core-shell particles.

Fig. 23 clearly shows the holes of grafted NR/PS semi-IPN-based particles which did not cavitate. On the other hand, fractured non-grafted rubber particles can be seen in Fig. 24. The magnification made it possible to see even the hard PS subinclusion nodules within the fractured natural rubber core.

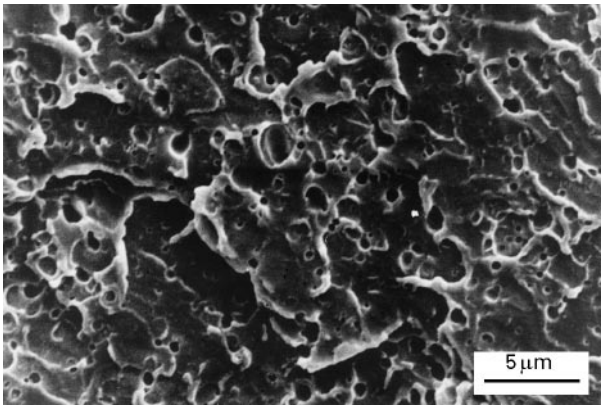

Figure 23 SEM photomicrograph of the notched Izod fracture surface of a PS blend containing 13 wt % core-shell particles based on grafted (t-BuHP/DMA initiation) 80 wt % natural rubber/20 wt % crosslinked PS latex semi-IPNs (core/shell ratio: 75/25, 15 wt % subinclusions).

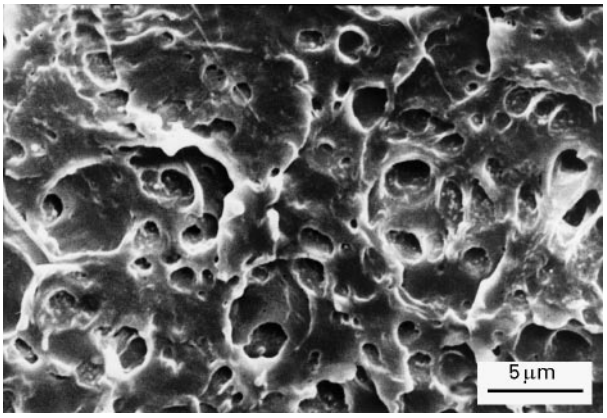

Figure 24 SEM photomicrograph of the notched Izod fracture surface of a PS blend containing 13 wt % core-shell particles based on non-grafted (AIBN initiation) 80 wt % natural rubber/20 wt % crosslinked PS latex semi-IPNs (core/shell ratio: 75/25, 15 wt % subinclusions).

In order to study the behaviour of high impact PS blends, 27 wt % grafted and non-grafted NR-based composite particles with 15 and 30 wt % subinclusions were incorporated into PS blends. Their impact resistance is compared in Fig. 25.

Fig. 25 shows that using t-BuHP/DMA initiation for the subinclusion synthesis yielded grafted NR/crosslinked PS semi-IPN-based latex particles containing 30 wt % PS subinclusions which were ineffective in toughening the PS matrix. The few nucleated crazes failed and premature matrix fracture was caused. At only 15 wt % PS subinclusions in the rubber core, grafted and non-grafted NR-based particles were equally effective, because the modulus increase of the grafted NR-based particles did not yet impede the craze preceding rubber cavitation [26, 44]. Examination of the notched Izod fracture surfaces of the prepared PS blends containing grafted (Fig. 23) and non-grafted (Fig. 24) NR/crosslinked PS semi-IPN-based core-shell particles indicate that grafted NR particles indeed did not cavitate. Rubber particles containing only 15 wt % PS subinclusions were more effective because grafting of NR chains could not be completely avoided at 30 wt % crosslinked PS

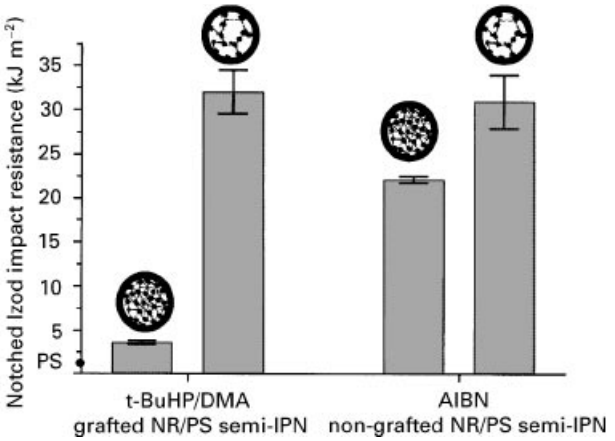

Figure 25 Dependence of impact resistance of high impact PS blends on the degree of grafting of NR/crosslinked PS semi-IPNs based core-shell particles containing 15 or 30 wt % crosslinked PS subinclusions and 25 wt % crosslinked PMMA in the shell (27 wt % particles in the blends).

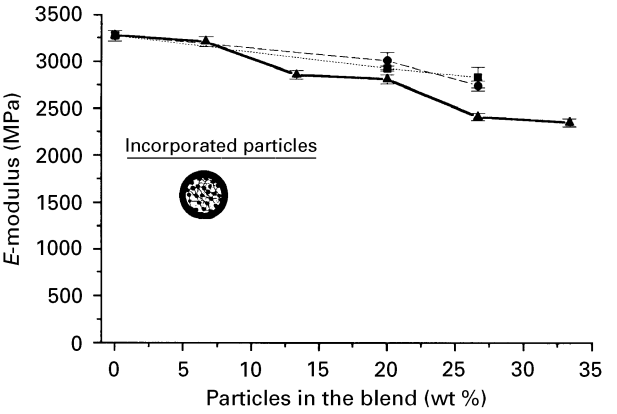

Figure 26 Dependence of the *E*-modulus of PS blends on the degree grafting of the incorporated NR/crosslinked PS semi-IPN-based core-shell particles containing 30 wt % crosslinked PS subinclusions within the NR core and 25 wt % crosslinked PMMA in the shell. (▲) non-grafted IPN (AIBN initiation at 70 °C); (■) grafted IPN (t-BuWP/DMA initiation); (●) grafted IPN (AIBN initiation at 85 °C).

subinclusions within the rubber core during emulsion polymerization. Besides, high PS amounts which lead to large PS subinclusions within the rubber core decrease the effectiveness of the incorporated core-shell particles as already discussed.

3.7.2. Tensile behaviour

Grafted NR-based composite latex particles could not toughen PS blends at fast deformation speeds. In order to analyse whether slow deformation speeds permit further differentiation between composite latex particles, tensile testing was performed on latex semi-IPNs with different degrees of grafting. Fig. 26 presents the *E*-modulus of PS blends containing different mass fractions of grafted or non-grafted latex semi-IPN-based particles.

Grafted NR-based particles slightly increased the modulus of the PS blends. A linear decrease of the *E*-modulus of the PS blends with the weight fraction of the incorporated composite particles could be established in Fig. 26.

Fig. 27 illustrates the decrease of the yield stress for the matrix deformation in the case of non-grafted NR-based particles (low modulus) in comparison with grafted NR-based latexes (high modulus). For better clarity only the deformation zone between 0 and 10% of ASTM standard dumbbell samples is shown. All PS blends contained 13 wt % particles. The bold lines represent the stress–strain properties of PS blends containing particles with 30 wt % PS subinclusions and the thin lines represent PS blends containing particles with only 15 wt % subinclusions. As indicated in Fig. 27, the systems for the synthesis of the PS subinclusions comprise AIBN initiation at 70 °C which generally does not graft NR chains and the redox initiating system t-BuHP/DMA at 50 °C, which grafts NR.

Comparing the stress–strain properties of PS blends containing either grafted or non-grafted NR-based composite particles illustrates how grafting raised the yield stress of the prepared PS blends containing mor-

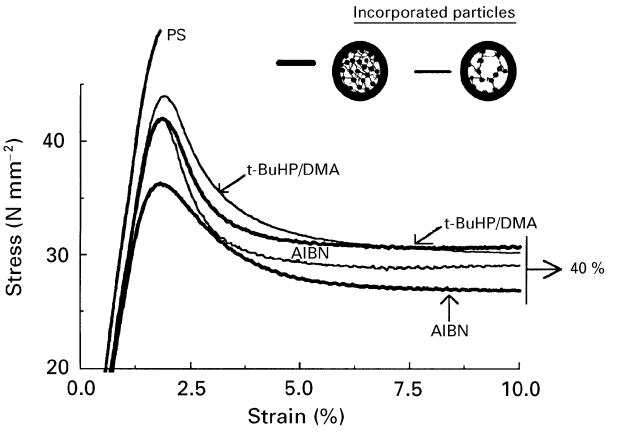

Figure 27 Dependence of the yield stress of PS blends on the degree grafting of NR/crosslinked PS semi-IPN-based core-shell particles containing 15 or 30 wt % crosslinked PS subinclusions within the rubber core and 25 wt % crosslinked PMMA in the shell.

phologically identical rubber particles. The effect is more pronounced for rubber particles with a high PS mass fraction in the rubber core. Polymerizing much styrene monomer within the natural rubber core affects the properties of the rubber phase to a large degree. Although the use of grafted high modulus NR-based particles increased the yield stress, extensive crazing allowed all PS blends to be elongated to about 40% at slow deformation speeds. The toughening efficiency of the four types of occluded core-shell particles could be well differentiated only by impact testing at fast loading rates. This is related to a rise of the minimum effective particle size. It is known that the critical particle diameter for the toughening of HIPS increases from 0.1 μm at slow deformation rates to about 0.4 μm at impact conditions [46]. Hence, especially submicrometer sized composite NR-based particles become ineffective when other factors such as grafting or large sized rigid subinclusions decrease their craze initiating and craze stabilizing capacity. Fig. 1 shows that more than 97% of the NR-based composite latex particles are smaller than 1 μm.

4. Conclusions

In this study the influence of the internal structure of natural rubber (NR)-based core-shell particles on the mechanical properties of PS blends was examined. All composite NR-based particles were incorporated as a wet latex directly into a co-rotating twin screw extruder which ensured a good dispersion of hard and also soft latex particles. At slow deformation speeds (tensile testing) a hard shell, rigid subinclusions and core-shell particles containing small or large sized subinclusions were equally effective in decreasing the yield stress of the PS matrix which could be elongated to 60%. High deformation speeds (impact testing) were necessary for the evaluation of the different impact modifiers for PS. The results indicate that several factors have to be kept in mind for most effective rubber toughening. The use of tailor-made preformed latex particles made it possible to study each factor separately.

1. Subinclusions alone did not render rubber particles capable of reinforcing PS. A hard shell was essential. Twenty-five weight per cent crosslinked PMMA in the particle were required for the formation of an intact hard shell around a soft natural rubber core.

2. A large number of small PS subinclusions changed the deformation mechanism at impact by improved rubber fibrillation which prevented premature fracture. Raising the mass fraction of the PS subinclusions within the rubber core increased the size of the subinclusions but did not alter the rubber fibrillation and crazing mechanism further.

3. Higher PS/natural rubber weight ratios in the core increased the yield stress of the PS blends. It is suggested that the increased modulus of the incorporated particles shifts the craze preceding rubber cavitation to higher stresses.

4. The degree of crosslinking of the PS subinclusions within the NR-based core-shell particles influenced the mechanical properties of PS blends indirectly by a change of the morphology of the occluded rubber core.

5. Low temperature and AIBN initiation for the preparation of the composite rubber particles were important in order to avoid excessive grafting of the natural rubber chains. Grafted NR-based particles did not toughen PS under impact conditions since high modulus rubber particles are less effective to initiate a large number of crazes. Furthermore, high temperature during the emulsion polymerization adversely influenced the performance of the composite rubber particles by an increase of the subinclusion size.

6. From the fracture surface morphology the craze nucleating and stabilizing efficiency of composite NR particles having different morphologies and grafting degrees could be deduced.

The very versatile emulsion polymerization procedures used for the preparation of composite natural rubber based toughening particles provided control over their morphology and modulus. These two factors determined the mechanical properties of PS blends containing such particles.

Acknowledgements

The authors would like to take this opportunity to thank the European Union for financing this research project (BRITE-EURAM Project BE-4260). They are grateful to the German Plastics Institute in Darmstadt for much advice concerning the optimized wet latex feeding on the extruder. The assistance of Mr Morvan of the Centre de Géochimie de la Surface in Strasbourg for the transmission electron studies is also gratefully acknowledged.

References

1. C. B. BUCKNALL, "Toughened plastics" (Applied Science Publishers, London, 1977).
2. M. SCHNEIDER, T. PITH and M. LAMBLA, in Proceedings of the International Conference on Multi-Phase Materials prepared by Emulsion Polymerisation, Lancaster University, UK, 4–7 April, 1995.
3. A. A. COLLYER, "Rubber toughened engineering plastics" (Chapman & Hall, London, 1994).
4. C. B. BUCKNALL and R. R. SMITH, *Polymer* **6** (1965) 437.
5. C. B. BUCKNALL and D. CLAYTON, *J. Mater. Sci.* **7** (1972) 202.
6. D. G. COOK, A. PLUMTREE and A. RUDIN, *Plast. Rubb. Comp. Proc. Appl.* **20** (1993) 219.
7. M. OKUBO, *Makromol. Chem. Macromol. Symp.* **35/36** (1990) 307.
8. S. SHEN, M. S. EL-AASSER, V. L. DIMONIE, J. W. VANDERHOFF and E. D. SUDOL, *J. Appl. Polym. Sci., Part A: Polym. Chem.* **29** (1991) 857.
9. F. VAZQUEZ, H. CARTIER, K. LANDFESTER, G.-H. HU, T. PITH and M. LAMBLA, *Polym. Adv. Technol.* **8** (1995) 309.
10. H. KESKKULA, D. A. MAASS and K. M. MCGREEDY, US Patent 4,460,744 (to Dow), July 17 (1984).
11. T. D. GOLDMAN, US Patent 4,443,585 (to Rohm and Haas), April 17 (1984).
12. C. KEITH RIEW and A. J. KINLOCH (eds), "Toughened plastics I: Science and engineering", Advances In Chemistry Series 233 (American Chemical Society, Washington, DC, 1993) p. 61.
13. M. SCHNEIDER, T. PITH and M. LAMBLA, *J. Mater. Sci.* **32** (1997) 6343–6356.
14. *Idem., Polym. Adv. Technol.* **8** (1995) 326.
15. S. WU, *Polym. Engng. Sci.* **30** (1990) 753.
16. R. J. CERESA, "Block and graft copolymerization", Vol. **1** (Wiley-Interscience Publication, London, 1973) p. 47.
17. P. W. ALLEN, G. AYREY, C. G. MOORE and J. SCANLAN, *J. Polym. Sci.* **36** (1959) 55.
18. M. SCHNEIDER, T. PITH and M. LAMBLA, *J. Appl. Polym. Sci.* **62** (1996) 273.
19. L. BATEMAN (ed.), "The chemistry and physics of rubber-like substances" (Maclaren, London, 1963) p. 97.
20. G. F. BLOOMFIELD and P. MCL. SWIFT, *J. Appl. Chem.* **5** (1955) 609.
21. D. J. HOURSTON and J. ROMAINE, *J. Appl. Polym. Sci.* **39** (1990) 1587.
22. K. KATO, *J. Electron Microsc.* **14** (1965) 220.
23. *Idem., Polym. Lett* **4** (1966) 35.
24. W. DÖLL, in "Fractography and failure mechanism of polymers and composites," ed. by A. C. Roulin–Moloney (Elsevier Applied Science London, New York, 1989) p. 387.
25. A. LAZZERI and C. B. BUCKNALL, *J. Mater. Sci.* **28** (1993) 6799.
26. C. B. BUCKNALL, A. KARPODINIS and X. C. ZHANG, *ibid.* **29** (1994) 3377.
27. A. M. DONALD and E. J. KRAMER, *J. Appl. Polym. Sci.* **27** (1982) 3729.
28. *Idem., J. Mater. Sci.* **17** (1982) 2351.
29. M. SCHNEIDER, T. PITH and M. LAMBLA, *J. Mater. Sci.* **32** (1997) 6331–6342.

30. A. BRYDON, G. M. BURNETT and G. G. CAMERON, *J. Polym. Sci.* **2** (1973) 3255.
31. G. G. CAMERON and M. Y. QURESHI, *ibid.* **18** (1980) 2143.
32. D. J. HOURSTON and J. ROMAINE, *J. Appl. Polym. Sci.* **43** (1991) 2207.
33. H. R. SHEU, M. S. EL-ASSER and J. W. VANDERHOFF, *J. Polym. Sci. A* **28** (1990) 629.
34. S. NISHI and T. KOTAKA, *Macromolecules* **18** (1985) 1519.
35. R. A. HAYES, *J. Polym. Sci.* **11** (1953) 531.
36. G. SMETS and M. CLAESEN, *ibid.* **8** (1952) 289.
37. R. A. GREGG and F. R. MAYO, *J. Amer. Chem. Soc.* **75** (1953) 3530.
38. G. H. MICHLER, *Makromol. Chem., Macromol. Symp.* **38** (1990) 195.
39. *Idem., Plast. Kautschuk*, **26** (1979) 680.
40. *Idem., ibid.* **35** (1988) 347.
41. D. DOMPAS and G. GROENINCKX, *Polymer* **35** (1994) 4743.
42. *Idem., ibid.* **35** (1994) 4750.
43. *Idem., ibid.* **35** (1994) 4760.
44. K. DIJKSTRA, A. VAN DER WAL and R. J. GAYMANS, *J. Mater. Sci.* **29** (1994) 3489.
45. R. A. BUBECK, D. J. BUCKLEY and E. J. KRAMER, *ibid.* **26** (1991) 6249.
46. G. H. MICHLER, B. HAMANN and J. RUNGE, *Angew. Makromol. Chem.* **180** (1990) 169.

Received 8 August 1995
and accepted 9 May 1997